JOURNAL OF MATERIALS SCIENCE 26 (1991) 6113–6118

Electrochemical method for the investigation of transport properties of alumina scales formed by oxidation

Part I *Theory*

D. NICOLAS-CHAUBET, A. M. HUNTZ, F. MILLOT
Institut de Science des Matériaux, Université Paris XI, 91405 Orsay, France

An electrochemical method is applied to the study of the transport properties of α-alumina scales developed by oxidation of alumina-forming alloys. This technique consists in plotting the characteristic curves *V* versus *I* of the scale. In this paper, relationships between the transport properties (σ_i, σ_e, t_i, . . .) of the scale and the variations of *V* with *I* are analysed and discussed. Information about the conductivity variation in the oxygen chemical potential gradient of the scale can be obtained from the slopes of *V–I* curves and from the evolution of such curves for different outer P_{O_2} imposed to the oxide. This method will be applied to α-alumina developed by oxidation of a β-NiAl alloy in part II.

1. Introduction

Alumina scales developed by oxidation are a protective coating for numerous refractory materials used in aggressive atmospheres. However, the growth mechanisms and the nature of diffusing species in alumina are still discussed. The transport properties, responsible at least for an important part of the protective characteristics of the oxide, are not yet well known [1].

Study of the transport properties of alumina scales is difficult, on the one hand, because of the extrinsic character of the transport properties of alumina (essentially linked to the presence of various impurities), and on the other hand, because of the physico-chemical specificity of corrosion scales: an oxide scale is subjected to chemical potential and electrical gradients, and possible impurity concentration gradients.

Because of this particularity of oxide scales, it appeared necessary to study the transport properties of corrosion scales at high temperature, in the real conditions of oxidation. An electrochemical method was chosen to study transport in thermal alumina scales. This method is based on the plot of the characteristic current–potential curves obtained in the oxide.

2. Statement of the problem

The use of electrical measurements in studying the transport properties of oxide scales is not new: the first experiments on the effect of an external electrical field on oxidation were performed in 1955 [2]. The application of such a method, especially to alumina, is more recent (1974–1978), with the work of Sheasby and co-workers [3, 4] and Dils and Follansbee [5]. More recently, Ben Abderrazik and co-workers used a similar method to study the transport properties of alumina scales developed by oxidation of commercial and laboratory FeCrAl alloys [6, 7].

The principle of the electrochemical experiments consists in imposing a potential difference, *V*, between the outer and the inner interfaces of the oxide scale, and then, in measuring the stationary electrical current *I* that crosses the scale. Then, from the *V–I* curves so determined, some information was obtained by the previously mentioned authors.

The potential difference, V_0, existing between the two interfaces of the growing scale (for $I = 0$), can be related to the ionic transport number t_i, with the generalized Nernst–Einstein equation:

$$V_0 = \frac{1}{4F}\int_{\mu_{in}}^{\mu_{out}} t_i \mathrm{d}\mu \qquad (1)$$

where μ_{out} and μ_{in} are the oxygen chemical potentials at the outer and inner interfaces, respectively, and $t_i = \sigma_i/\sigma$, the ratio of the ionic conductivity, σ_i, and of the total electric conductivity, σ.

An example of a characteristic curve obtained with alumina is represented in Fig. 1 (from Ben Abderrazik *et al.* [6]). The linear part of the *V–I* curve was attributed to an ohmic behaviour of the alumina scale, and so the slope gave the average resistance of the scale. From the average ionic transport number obtained with Equation 1, and from the average total conductivity, the average ionic conductivity was deduced: $\bar{\sigma}_i = \bar{t}_i\,\bar{\sigma}$.

Using such an analysis, Sheasby and Jory [3] showed that alumina formed on a Pt–Al alloy behaves as a mixed conductor ($t_i \simeq 0.5$). Ben Abderrazik *et al.* [7] obtained a similar result with alumina scales grown on an FeCrAl alloy. In contrast, Dils and Follansbee [5] showed that for alumina developed by

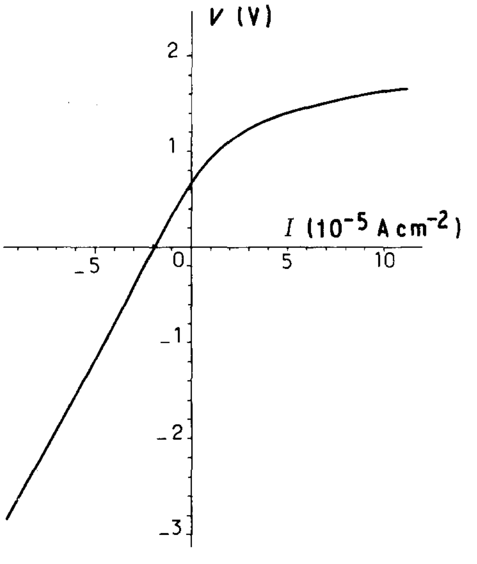

Figure 1 V–I curve obtained with an alumina scale formed on a laboratory FeCrAl alloy oxidized for 20 h at 1080 °C in pure oxygen [6].

an FeCrAlY alloy, the scale behaves like an electronic conductor ($t_i \simeq 10^{-2}$).

However, it must be remarked that values so determined only represent the average transport properties in the scale. It would certainly be interesting to know more about the variation of conduction properties inside the scale, particularly versus the oxygen chemical potential. From a knowledge of the functions $\sigma_i = f(P_{O_2})$ or $\sigma_e = f(P_{O_2})$, a model of defect transport could be imagined (σ_e is the electronic conductivity). And so it could be possible to identify the nature of the species that mainly ensure the transport during oxidation. To that end, the relationships between the transport properties of the scale and the variations of V and I have to be precisely determined.

The previous authors [3, 5, 6, 7] were not very interested by the shape of the curves, in spite of the fact that they all observed an asymmetry of the V–I curves determined for alumina. However, they proposed explanations for the deviation from ohmic behaviour observed for positive values of V and I:

(i) Dils and Follansbee [5] suggested a diode effect attributed to the Pt–Al_2O_3–substrate junction.

(ii) Ben Abderrazik *et al.* [7] proposed a diode effect inside the alumina scale. Referring to the numerous studies on synthetic alumina showing that it behaves as an n-type conductor for low oxygen partial pressures and as a p-type conductor for the high ones, they made the assumption of an n–p junction in the scale, leading to a diode effect. Ben Abderrazik previously showed that the phenomenon studied has to be attributed to the volume of alumina scale: the apparent measured resistance is proportional to the thickness of the scale. This indicates that the polarization of interfaces is negligible [8–16].

This diode effect does not seem satisfactory, for two reasons:

(i) it supposes the existence, inside the scale, of an area where local equilibrium is not realised; and

(ii) the high value determined for V_0 (between 0.5 and 1 V), necessary for the appearance of the deviation from ohmic behaviour, excludes an electronic effect (of diode type) explaining the shape of the curve.

A more attractive explanation is given by Sheasby and Jory [3], who suggest that the deviation from linearity of the curve is linked to the oxygen chemical potential gradient inside the scale that compensates the applied electrical potential difference.

But as neither a satisfactory interpretation nor real study of the shape of the V–I curves existed for such corrosion scales, it appeared necessary to make a theoretical approach to the physical information contained in the shape of such curves. It must be noted that theoretical approaches to current–potential relationships have been made for solid electrolytes subjected to oxygen potential gradients [17–20], cases comparable to that of alumina scales.

3. Theoretical approach to the shape of *V–I* curves obtained on alumina

The details of the formalism allowing one to establish the expressions for V, I and dV/dI, are more familiar to electrochemists than to metallurgists, but they will not be fully described here.

3.1. Description of the system and principle of measurements

The system studied is a pure alumina scale, of thickness Z_{ox}, formed by the oxidation of an alloy (in order to impose fixed aluminium and oxygen chemical potential at the inner interface). The scale is subjected to oxygen and aluminium chemical potential gradients and to an electrical potential gradient. Under the influence of these forces, transport phenomena occur.

A platinum electrode, of surface S, is in contact with the upper side of the oxide. The other electrode is in contact with substrate whose resistance is neglected. These electrodes are connected to the external electrical circuit by platinum wires. The external circuit allows one to impose an electrical current on the alumina scale (Fig. 2).

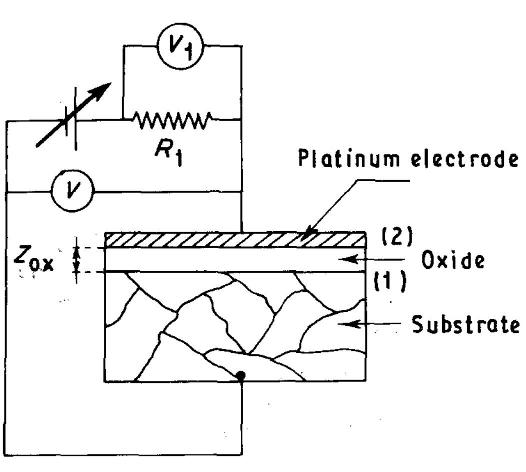

Figure 2 Equivalent electrical circuit used to determine V–I curves.

3.2. Assumptions

(i) Only charged species contribute to transport (Al^{3+}, O^{2-}, n, p);

(ii) electrodes are reversible both to electrons and ions (i.e. equilibrium is realised at each interface);

(iii) applied forces are small compared to interionic forces;

(iv) local equilibrium is assumed and local thermodynamic quantities are defined;

(v) geometry is unidimensional and temperature is uniform.

It can be remarked here that the assumption of interface equilibrium is realistic in our case, as Ben Abderrazik previously showed that interface polarization could be neglected [8–16].

3.3. Basic equations

The potential difference between the two opposite faces (1 and 2) of the scale is related to the electrochemical potential gradient of the electrons $\nabla\eta_n$:

$$V = -\frac{1}{F}\int_1^2 d\eta_n \qquad (2)$$

The gradient of partial pressures of oxygen is related to the gradient of oxygen chemical potential:

$$\nabla\mu_{O_2} = RT\nabla(\ln P_{O_2}) \qquad (3)$$

For any mobile species k, we shall write the following relation between the flux J_k and the electrochemical gradient $\nabla\eta_k$:

$$J_k = -\frac{\sigma_k}{Z_k^2F^2}\nabla\eta_k \qquad (4)$$

where σ_k and Z_k are the conductivity and the charge of k, respectively. F is the Faraday number.

It must be noted that, in such an experiment, the electronic (n or p) species cannot be distinguished between themselves. It is the same for ionic species (Al^{3+} and O^{2-}). So electronic and ionic quantities are defined:

$$J_i = 3J_{Al^{3+}} - 2J_{O^{2-}} \quad \text{(ionic flux)} \qquad (5)$$

$$J_e = J_p - J_n \quad \text{(electronic flux)} \qquad (6)$$

$$\sigma_i = \sigma_{Al^{3+}} + \sigma_{O^{2-}} \quad \text{(ionic conductivity)} \qquad (7)$$

$$\sigma_e = \sigma_n + \sigma_p \quad \text{(electronic conductivity)} \qquad (8)$$

From the assumption of local equilibrium, and of virtual equilibrium, the following equations can be established:

$$J_i = \frac{\sigma_i}{4F^2}\nabla\mu_{O_2} + \frac{\sigma_i}{4F^2}\nabla\eta_n \qquad (9)$$

$$J_e = \frac{\sigma_e}{F^2}\nabla\eta_n \qquad (10)$$

$$I = -SF(J_i + J_e) \qquad (11)$$

In order to write more easily the following equations, μ_{O_2} and η_n will now be noted μ and η, respectively.

3.4. Current-voltage relations

From Equations 2 and 9–11 it has been possible to establish expressions for V, I and dV/dI for a stationary state of electromigration [21, 22], using $\alpha = J_i/J_e$ as a parameter:

$$V = \frac{-1}{4F}\int_1^2\left(\alpha\frac{\sigma_e}{\sigma_i} - 1\right)^{-1} d\mu \qquad (12)$$

$$I = \frac{S}{4FZ_{ox}}(\alpha + 1)\int_1^2\left(\frac{1}{\sigma_e} - \frac{\alpha}{\sigma_i}\right)^{-1} d\mu \qquad (13)$$

Equations 12 and 13 constitute the parametric representation of the current–voltage relation where α can take all possible values except $]\min(\sigma_i/\sigma_e), \max(\sigma_i/\sigma_e)[$.

From Equations 12 and 13, dV/dI is calculated:

$$\frac{dV}{dI} = \frac{Z_{ox}}{S}$$

$$\int_1^2 \frac{t_i(1 - t_i)}{[\alpha(1 - t_i) - t_i]^2}d\mu \Big/ \int_1^2 \frac{\sigma t_i(1 - t_i)}{[\alpha(1 - t_i) - t_i]^2}d\mu \qquad (14)$$

It has been shown from Equation 14 that the V–I curve approaches asymptotes whose slopes are equal to $Z_{ox}/S(\sigma_i^* + \sigma_e^*)$, with σ_i^* and σ_e^* the values of σ_i and σ_e for Min or Max(σ_i/σ_e), respectively, according to the asymptote considered [21, 22].

4. Relations between the shape of V–I curves and transport property variations in the oxygen chemical potential gradient inside the scale

An example of a V–I curve is plotted in Fig. 3 with the variations of the parameter α. As α goes from $]\mathrm{Max}(\sigma_i/\sigma_e), +\infty[,]-\infty, \mathrm{Min}(\sigma_i/\sigma_e[$, V and I go from negative to positive values. Table I collects the values of V, I, and dV/dI for a few particular points.

Some known results are found: if no current is imposed on the alumina scale by the external electrical circuit, the potential difference, V_0, between the inner and the outer interfaces is given by the generalized Nernst–Einstein relation (Equation 1):

$$V_0 = \frac{1}{4F}\int_{\mu_1}^{\mu_2} t_i d\mu \qquad (15)$$

From the determination of V_0 for different oxygen partial pressures, $\mu^{(2)}$, imposed on the oxide, it is possible to determine $\bar{t}_i(\mu^{(2)})$, a function whose differentiation gives $t_i(\mu)$.

Overall, Table I shows the close relationships between the shape of current–potential curves and the conductivity variations with the oxygen chemical potential gradient inside the scale. The slope dV/dI is inversely proportional to a conductivity weighted by a function of t_i and α. Considering the particular points of the V–I curves, the weighting function strongly promotes conductivity corresponding to high, medium or low t_i values:

(i) The slope of asymptotes is inversely proportional to the value of the conductivity for Min or Max(σ_i/σ_e).

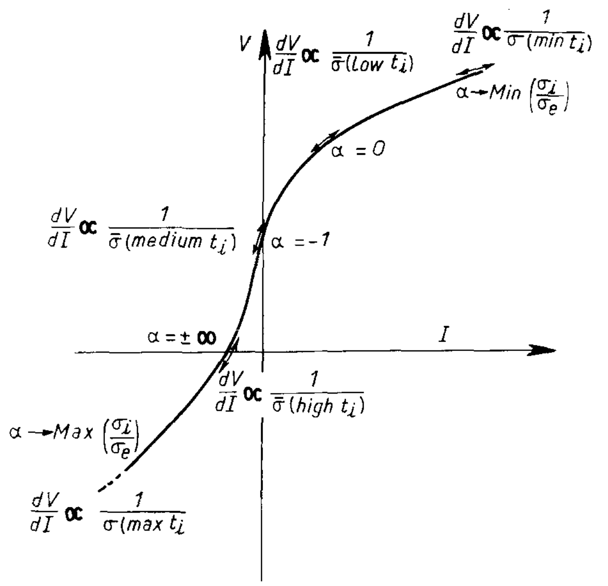

Figure 3 Shape of a *V–I* curve with the variation of the slopes versus parameters $\alpha (\alpha = J_i/J_e)$.

TABLE I Characteristic properties of some particular points of *V–I* curves

α	I	V	$\frac{Z_{\text{OX}}}{S}\frac{\mathrm{d}V}{\mathrm{d}I}$
$\alpha \rightarrow \text{Max}\left(\frac{\sigma_i}{\sigma_e}\right)$	$-\infty$	$-\infty$	$\frac{1}{\sigma(\text{Max}\, t_i)}$ asymptote
$\alpha \rightarrow \pm\infty$	$\frac{S}{4FZ_{\text{OX}}}\int_1^2 -\sigma_i \mathrm{d}\mu$	0	$\frac{\int_1^2 \frac{t_i}{1-t_i}\mathrm{d}\mu}{\int_1^2 \sigma\frac{t_i}{1-t_i}\mathrm{d}\mu}$
-1	0	$V_0 = \int_1^2 \frac{t_i}{4F}\mathrm{d}\mu$	$\frac{\int_1^2 t_i(1-t_i)\mathrm{d}\mu}{\int_1^2 \sigma t_i(1-t_i)\mathrm{d}\mu}$
0	$\frac{S}{4FZ_{\text{OX}}}\int_1^2 \sigma_e \mathrm{d}\mu$	$\frac{\mu^2-\mu^1}{4F}$	$\frac{\int_1^2 \frac{1-t_i}{t_i}\mathrm{d}\mu}{\int_1^2 \sigma\frac{1-t_i}{t_i}\mathrm{d}\mu}$
$\alpha \rightarrow \text{Min}\left(\frac{\sigma_i}{\sigma_e}\right)$	$+\infty$	$+\infty$	$\frac{1}{\sigma(\text{Min}\, t_i)}$ asymptote

(ii) From the domain of V and I negative values to the domain of V and I positive values, the slope of a *V–I* curve is successively inversely proportional to the conductivity for $\text{Max}(t_i)$, then to the average conductivity for high t_i, and medium t_i, and low t_i, and then to the conductivity for $\text{Min}(t_i)$ (see Fig. 3).

(iii) It can be observed that negative values of V and I are associated with slopes inversely proportional to the average conductivity for high t_i values. So, this branch of the *V–I* curve was called the "ionic branch". By analogy the branch where V and I are positive was called the "electronic branch".

Then, it is possible to link the variation of the slope of a characteristic curve to the variations of the total conductivity, σ, of the ionic conductivity, σ_i, and of the electronic conductivity, σ_e, in the oxygen chemical potential gradient existing in alumina.

Let us consider the example of the characteristic curve of Fig. 3: slopes for V and I negative values are higher than slopes for V and I positive values: the average total conductivity $\bar{\sigma}$ for high t_i is lower than the average total conductivity for low t_i. Moreover, between the two particular points $V = 0$ and $I = 0$, the slope increase is about twice. So, the conductivity does not vary largely between the electronic and the ionic domains. A diagram as shown in Fig. 4 can be proposed to explain the shape of the *V–I* curve of Fig. 3.

A consequence of the relations between the shape of the *V–I* curves and conductivity variations, is that various *V–I* curves can be obtained according to the σ_i and σ_e variations versus μ, the oxygen chemical potential in the scale. Two examples are shown in Figs 5 and 6.

However, it should be remarked from Fig. 7 that inverse variations of σ_i and σ_e versus μ lead to the same *V–I* curve, and consequently that it is not possible to assess from a *V–I* curve a unique representation of conductivity variations. A tentative means to do so may consist of comparing various *V–I* curves obtained on changing $\mu^{(2)}$ values (i.e. by changing the outer oxygen partial pressure imposed on the oxide).

Fig. 8 shows inverse variations of σ_i and σ_e that can be associated with curve I of Fig. 9. Curves II of Fig. 9a and b illustrate the different evolutions of the characteristic curve when $\mu^{(2)}$ decreases for each of the inverse conductivity variations of Fig. 8a and b, respectively.

In case (a), as $\mu^{(2)}$ decreases the domain of dominant electronic conductivity is affected. Thus, $\sigma[\text{Min}(\sigma_i/\sigma_e)]$ decreases, and so does the slope of the asymptote for V and I positive values. As the domain of dominant ionic conductivity is not affected, the "ionic branch" is not modified.

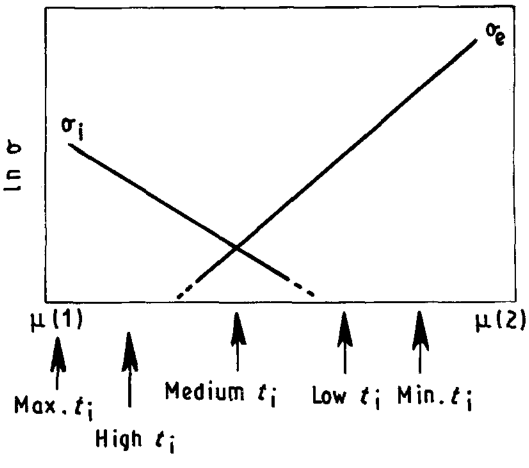

Figure 4 Possible variation of conductivity that can be related to the *V–I* curve of Fig. 3.

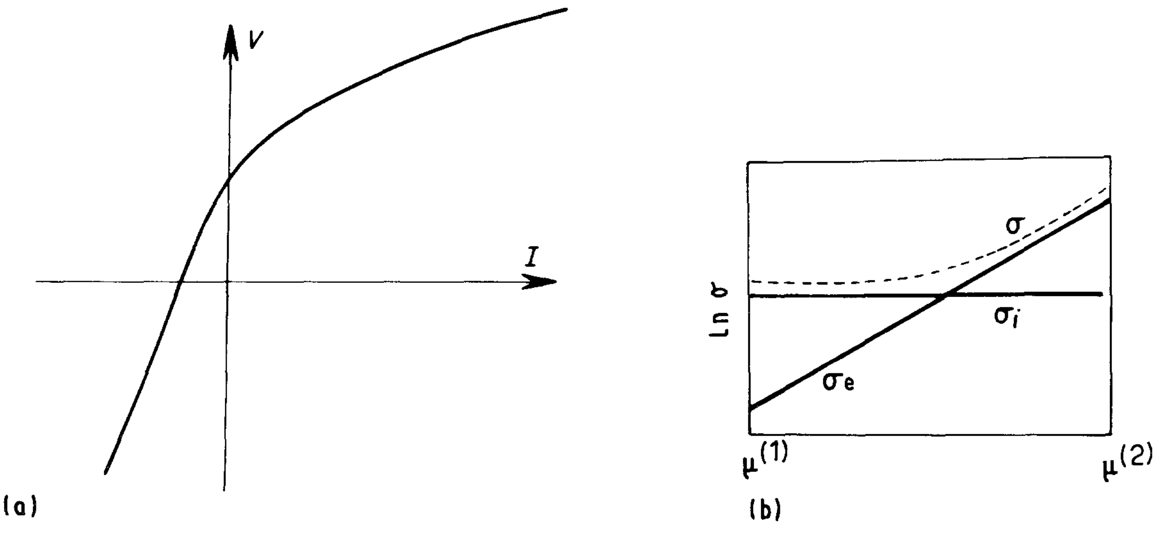

Figure 5 Example of associated (a) V–I and (b) conductivity variation curves.

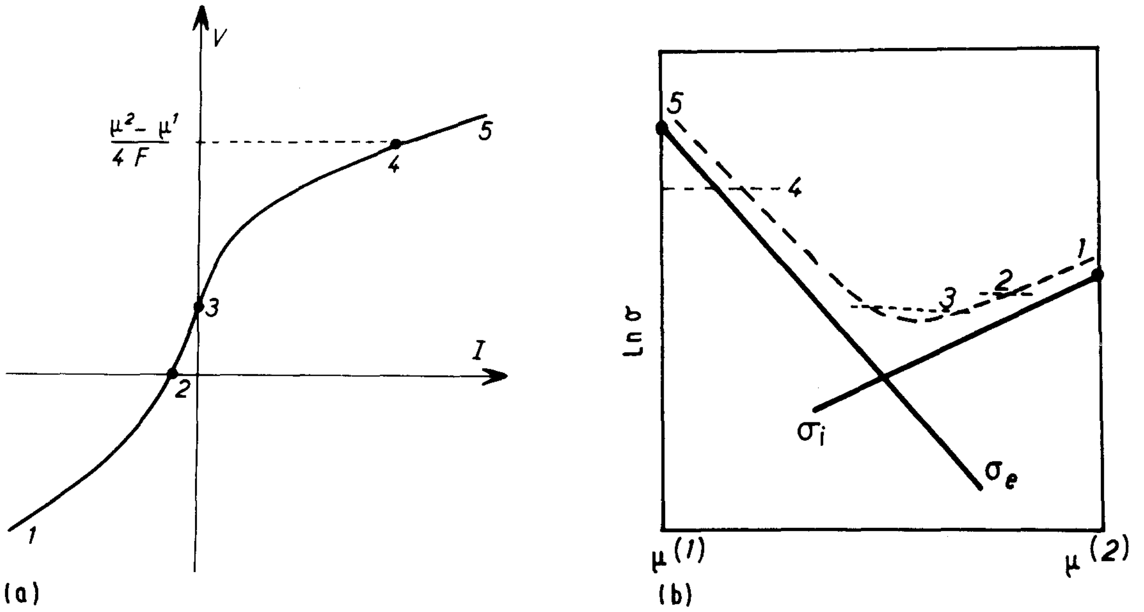

Figure 6 Another example of associated (a) V–I and (b) conductivity variation curves.

In case (b), as $\mu^{(2)}$ decreases the domain of dominant ionic conductivity is affected. But the variation of $\mathrm{Max}(\sigma_i/\sigma_e)$ is slight, and so there is little change of the slope of the "ionic branch". However, V_0 decreases, moving the V–I curve down.

These simplified examples show that a comparison of the evolution of the V–I curves obtained for different oxygen chemical potentials imposed on the scale can give access to the conductivity variation in the oxygen chemical potential gradient existing inside the alumina scale.

These conclusions can be applied to doped alumina or doped alumina in equilibrium with a second phase, provided that the dopant is in low concentration and is not involved in transport. Such a technique and its formalism will be applied in the second part of this paper to alumina scales developed by oxidation of a β-NiAl alloy at 1100 °C [21–23].

5. Conclusion

This work showed the interest of an electrochemical method for studying transport properties of alumina scales developed by oxidation of an alloy.

It appeared that from the analysis and a comparison of the characteristic V–I curves, obtained for different outer oxygen partial pressures imposed on an alumina scale, diagrams for the variation of the conductivity inside of the scale can be proposed. This goes far beyond the average descriptions previously obtained with electrical measurements on oxide scales.

Another practical advantage of electrical measurements is that they can be made on the oxide scale itself, and in the real conditions of oxidation.

This electrochemical method has been used in the study of transport properties of alumina formed by oxidation of a β-NiAl alloy at 1100 °C in oxygen [21–23].

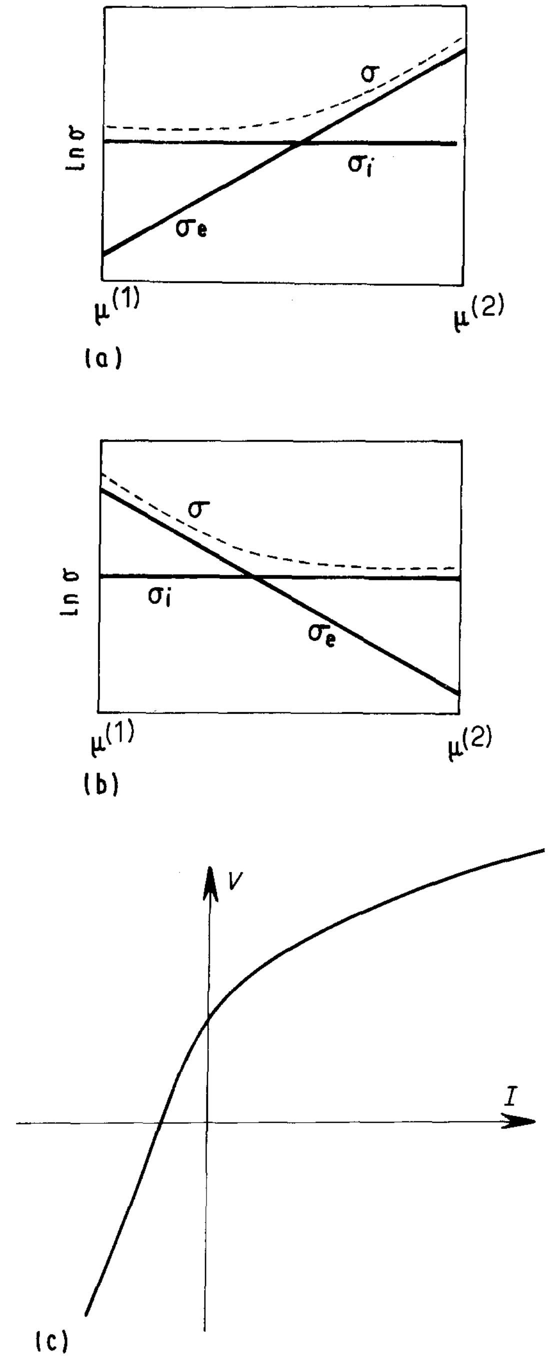

Figure 7 (a, b) Inverse variations of conductivity that may be associated with the same *V–I* curve (c).

References

1. A. M. HUNTZ, *Mater. Sci. Engng* **87** (1987) 251.
2. H. H. HULIG and A. E. BRENNER, *Acta. Metall.* **3** (1955) 108.
3. J. S. SHEASBY and D. B. JORY, *Oxid. Met.* **12** (1978) 527.
4. J. S. SHEASBY and J. D. GRANDSEN, in Proceedings of 6th Congress on Metal Corrosion, Sydney, Australia (1975) pp. 4–9.

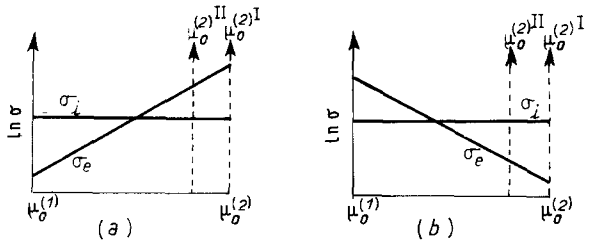

Figure 8 (a, b) Inverse variations of conductivity that may be associated with the *V–I* curve I of Fig. 9.

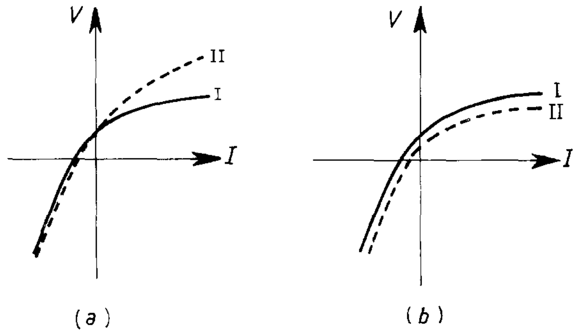

Figure 9 (a, b) Evolution of *V–I* curves as oxygen partial pressure decreases for the conductivity variations of Fig. 8a and b, respectively.

5. R. R. DILS and P. S. FOLLANSBEE, “Electronic and Ionic Conduction in Alumina Oxides Grown on High Temperature Alloys”, Pratt and Whitney Aircraft Report No. 74–005 (1974).
6. G. BEN ADBERRAZIK, F. MILLOT, G. MOULIN and A. M. HUNTZ, *J. Amer. Ceram. Soc.* **68** (1985) 302.
7. *Idem., ibid.* **68** (1985) 307.
8. G. BEN ABDERRAZIK, Doctoral thesis, University of Paris XI, Orsay (1986).
9. *Idem., Métaux Corrosion et Industrie* No. 733 (1986) 253.
10. *Idem., ibid.* No. 734 (1986) 291.
11. *Idem., ibid.* No. 735–6 (1986) 344.
12. *Idem., ibid.* No. 739 (1987) 73.
13. *Idem., ibid.* No. 740 (1987) 113.
14. *Idem., ibid.* No. 741 (1987) 173.
15. *Idem., ibid.* No. 743–4 (1987) 235.
16. *Idem., ibid.* No. 747–8 (1987) 358.
17. N. S. CHOUDHURY and J. W. PATTERSON, *J. Electrochem. Soc.* **118** (1971) 1398.
18. D. S. TANNHAUSER, *ibid.* **125** (1978) 1277.
19. I. RIESS, *ibid.* **128** (1981) 2077.
20. *Idem, J. Phys. Chem. Solids* **47** (1986) 129.
21. D. NICOLAS-CHAUBET, thesis, University of Paris XI, 812, Orsay (1989).
22. *Idem., Métaux Corrosion et Industrie* No. 763 (1989) 61; Nos 765, 766 (1989) 121; No. 768 (1989) 191.
23. D. NICOLAS-CHAUBET, A. M. HUNTZ and F. MILLOT, *J. Mater. Sci.* **26** (1991) in press.

Received 23 July 1990
and accepted 6 February 1991